

## Gap at the Fermi level in the intermetallic vacancy system $RNiSn$ ( $R = Ti, Zr, Hf$ )

F.G. Aliev, N.B. Brandt, V.V. Moshchalkov, V.V. Kozyrkov, R.V. Skolozdra,  
and A.I. Belogorokhov

Low Temperature Physics Laboratory, Department of Physics,  
Moscow State University, Moscow, USSR

Received July 6, 1988; revised version October 10, 1988

The new class of intermetallic compounds  $RNiSn$  ( $R = Ti, Zr, Hf$ ) may be characterised by the presence of an ordered sublattice of Ni atom vacancies in comparison with normal metals  $RNi_2Sn$  with no Ni vacancies. We report unusual transport and optical properties of the  $RNiSn$  system. The electrical resistivity of  $RNiSn$  is very high ( $3 < \rho < 100$ ) mOhm\*cm; the temperature coefficient of resistivity (TCR) is negative and strongly dependent on the annealing conditions. For some samples  $ZrNiSn$  and for a single crystal of  $TiNiSn$  the resistivity can be described by the Mott's law at temperatures  $0.1 < T < 20$  K. A phase transition near  $T = 100$  K without change of crystal structure was deduced from Hall effect data and the temperature dependence of the lattice constant. Preliminary data on transport phenomena in  $RPtSn$  and  $RPdSn$  ( $R = Ti, Zr, Hf$ ) compounds are also reported. The unusual properties of  $RNiSn$  system might be related to a gap of the electron spectrum near the Fermi energy.

### Introduction

The physical properties of compounds with an ordered lattice of vacancies have been intensively studied during last years. The main part of these studies is connected with semiconducting compounds [1], oxide systems such as HTSC [2], and only a few intermetallic compounds with vacancy lattices, for example  $LiAl$  [3], are known. The specific feature of  $LiAl$  is the presence of a Li atom's vacancies sublattice with a concentration up to 5–10%.

In this paper we present electric, optic and lattice properties of a new class of intermetallic compounds  $RNiSn$  ( $R = Ti, Zr, Hf$ ), in which the presence of an ordered sublattice of Ni atom's vacancies (in comparison with Heusler compound  $RNi_2Sn$ ) induces a gap in the energy spectrum of the electrons.

Heusler compounds have been intensively studied during last years because of their unusual magnetic properties. Most of these compounds are metallic and have chemical compositions  $MnX_2Y$  and  $MnXY$  with X typical In, Sn, Sb, Al, Ge, Ga and Y commonly Cu, Co, Ni, Pd, Pt, Rh (see for example [4, 5]). In  $MnNiSb$ ,  $MnPtS$  and some other Mn Heusler com-

pounds semimetallic ferromagnetism with a gap in the electron spectrum for the minority spin direction has been predicted by band structure calculations [6].

The crystal structure of  $RMSn$  consists of four interpenetrating fcc sublattices with positions  $A(000)$ ,  $B(1/4, 1/4, 1/4)$ ,  $C(1/2, 1/2, 1/2)$  and  $D(3/4, 3/4, 3/4)$  ( $MgAgAs$  type crystal structure with space group  $F43m$ ). A remarkable feature of  $RMSn$  is the emptiness of the  $C$  sublattice in the contrast to  $RM_2Sn$ . We have found that  $RM_2Sn$  may be considered as a normal metal, but the  $RMSn$  compounds belong to a new class of materials. Under proper annealing conditions the formation of a gap in electron energy spectrum near the Fermi level is observed in the  $RMSn$  system.

### Experiment

$RNiSn$  samples were prepared by arc melting together the appropriate amounts of 99.99% pure components in an argon atmosphere. Then these samples were annealed at 800 °C in vacuum for different times ranging from 1 h up to 4 weeks. Characterisation of samples by standard X-ray diffraction technique showed

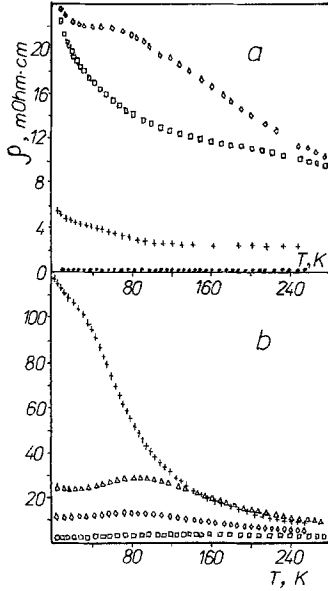


**Fig. 1.** **a** Temperature dependence of resistivity for HfNiSn ( $\diamond$ ), ZrNiSn ( $\square$ ) and TiNiSn ( $+$ ) and also for the reference compound ZrNi<sub>2</sub>Sn ( $\bullet$ ). **b**  $\rho(T)$  curves for ZrNiSn n.650 with different annealing time ( $\tau$ ) and the following  $(1-x)$  values: ( $\square - \tau = 0$ ,  $1-x = 0.68 \pm 0.13$ ); ( $+ - \tau = 200$  h,  $1-x = 0.83 \pm 0.07$ ); ( $\diamond - \tau = 340$  h,  $1-x = 0.8 \pm 0.11$ ); ( $\triangle - \tau = 680$  h,  $1-x = 0.8 \pm 0.06$ )

a well defined cubic structure with the lattice parameters corresponding to those found by Scolozdra et al. [7]. Resistivity, magnetoresistivity and Hall effect were measured with a micro-computer controlled four probe technique. Optical properties were studied on an infrared Fourier spectrometer "Brucker IFS-113 V".

Typical resistivity vs temperature curves of HfNiSn, ZrNiSn and TiNiSn compounds together with the reference compound ZrNi<sub>2</sub>Sn are shown in Fig. 1. In RNiSn the  $\rho(4.2$  K) value varies in the range  $3 < \rho < 100$  mOhm\*cm which is about three orders of magnitude higher than in the normal metallic ZrNi<sub>2</sub>Sn. The high resistivity value and the strong temperature dependence can not be due to the formation of microcracks in samples during cooling since the experimental  $\rho(T)$  data are quite reproducible under thermocycling. RNiSn samples exhibit a temperature independent Pauli paramagnetism. Therefore, the unusual  $\rho(T)$  behaviour cannot be explained by the presence of a magnetic transition either.

Another interesting feature of RNiSn samples is the drastic change of their properties after annealing. To understand the origin of this phenomenon, we studied a number of ZrNiSn samples with different annealing time (see Fig. 1b) and simultaneously performed computer simulation of the X-ray diffraction patterns. We have found that Ni atoms and empty C sublattice (Vac) are located on their regular posi-

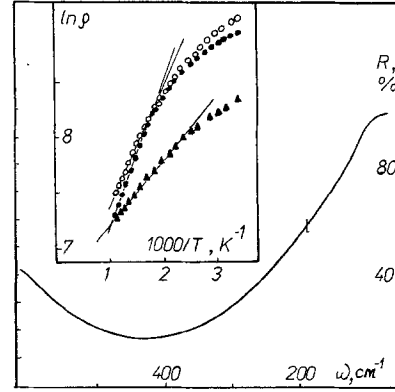


**Fig. 2.** Reflection coefficient  $R$  from Fourier spectra for ZrNiSn n.191 C at  $T = 300$  K. Insert shows  $\ln \rho = f(1000/T)$  for HfNiSn ( $\bullet$ ), ZrNiSn ( $\circ$ ) and TiNiSn ( $\blacktriangle$ )

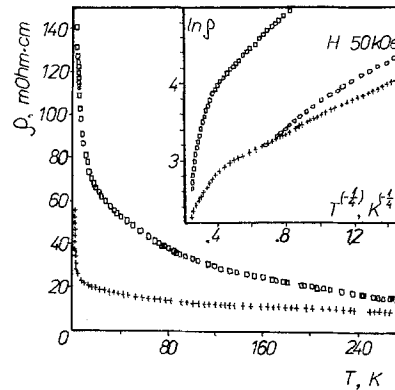
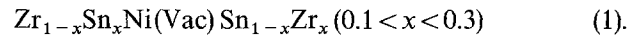


**Fig. 3.** Temperature dependence of resistivity  $\rho(T)$  for ZrNiSn n.191 C ( $+$ ) and monocrystalline TiNiSn N° 1 ( $\square$ ). The insert shows the  $\rho(T)$  dependence in coordinates  $\rho = f(T^{-1/4})$

tions, but Zr and Sn atoms substitute each other. In this situation the chemical formula of the RNiSn compound may be written as



Within the limits of the error in  $x$  (about 10%) we observed a correlation between the level of the substitutional disorder and the values of the negative TCR and resistivity (see Fig. 1b). The temperature dependence of the resistivity of RNiSn at ( $500 < T < 1000$ ) K correspond to a simple exponent  $\rho \approx \exp\left(\frac{\varepsilon_g}{2k_B T}\right)$  with

the gap parameter:  $\varepsilon_g(\text{HfNiSn}) \approx 220$  meV,  $\varepsilon_g(\text{ZrNiSn}) \approx 186$  meV,  $\varepsilon_g(\text{TiNiSn}) \approx 120$  meV (see insert on Fig. 2). On the other hand, for ZrNiSn N° 191 C and the TiNiSn monocrystal (see Fig. 3) we observed an agreement with Mott's law in the temperature range  $T < 30$  K:  $\rho = \rho_0 \cdot \exp(T_0/T)^{1/4}$ . In the temperature interval where Mott's law was obeyed, the magnetoresistance of ZrNiSn N° 191 is small and positive. It increases as  $T \rightarrow 0$  and it reaches  $\Delta\rho(50 \text{ kOe})/\rho(0) \approx 0.35$  for  $T \approx 0.2$  K (see insert in Fig. 3).

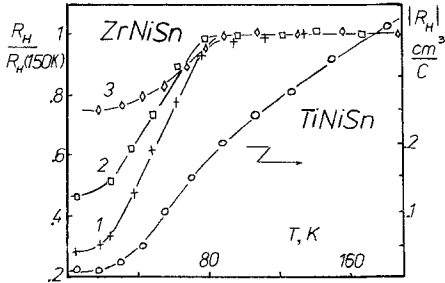


Fig. 4. Temperature dependences of the Hall coefficient  $R_H(T, H = 30 \text{ kOe})$  for ZrNiSn N° 191 with various annealing time at  $T \approx 800 \text{ C}^\circ$  (1–320 h, 2–350 h, 3–380 h) and for TiNiSn

Studying the Hall effect in ZrNiSn, we have found that in the best ordered samples (classified by the profile analysis of the X-ray pattern at  $T = 300 \text{ K}$ ), the Hall concentration is about  $(1-2) \cdot 10^{19} \text{ cm}^{-3}$  and the Hall mobility near  $(20-70) \text{ cm}^2/\text{B} \cdot \text{sec}$ . The temperature dependences of the Hall coefficient  $R_H(T)$  and of the lattice constant  $a(T)$  in ZrNiSn demonstrate a possible phase transition in ZrNiSn near  $T = 100 \text{ K}$  without a change of the crystal structure. Figure 4 shows the temperature dependences of the normalized Hall coefficient  $R_H(T)/R_H(150 \text{ K})$  for three samples ZrNiSn with various annealing times. A kink near  $T \approx 100 \text{ K}$  is detected for all samples. A computer simulation of the room temperature x-ray diffraction patterns shows the increase of symmetry of the environment of the vacancy sublattice from sample N° 1 to N° 3 (i.e. decrease of the  $x$  parameter in (1)). The temperature dependence of the lattice parameter  $a(T)$  shows a strong decrease near  $T \approx 100 \text{ K}$  (Fig. 5a). It should be mentioned that the amplitude of this transition is greater for less ordered samples. We did not find any anomaly in  $a(T)$  for HfNiSn and TiNiSn (Fig. 5b). In these compounds also the  $R_H(T)$  shows a smooth dependence on the temperature (Fig. 4). It is interesting to note that lowering the temperature induces metallic behaviour for  $R_H$  and gapping of spectrum from  $\rho(T)$  curve. This disagreement between  $R_H$  and  $\rho(T)$  data may be due to the presence of a wide transition in HfNiSn and TiNiSn compounds.

Infrared spectroscopy of the transmittance coefficient  $T(\omega)$  and of the reflectance  $R(\omega)$  in the RNiSn system was carried out at temperatures between 5 and 300 K and at frequencies from 20 up to  $4000 \text{ cm}^{-1}$ . The absorption coefficient  $\alpha(\omega)$  of ZrNiSn exhibits a minimum near  $\omega \approx 2000 \text{ cm}^{-1}$  which is in good correspondence with the gap value  $\varepsilon_g \approx 0.18 \text{ eV}$  derived from transport experiments. For some samples,  $R(\omega)$  shows a plasma minimum (for example  $\omega_p \approx 400 \text{ cm}^{-1}$  for ZrNiSn N° 191 C (see Fig. 2) or a strong anomaly in the  $R(\omega)$  and the  $T(\omega)$  spectra

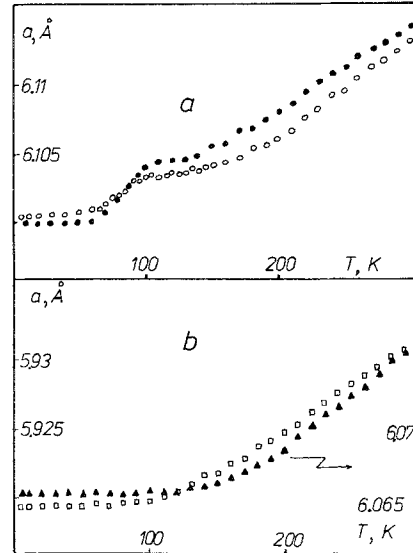


Fig. 5a and b. Lattice parameter (a) vs temperature in ZrNiSn N° 191 (380 h) (circles) and ZrNiSn N° 650 (340 h) (points) (a) and  $a(T)$  for HfNiSn (▲) and TiNiSn (□) on b

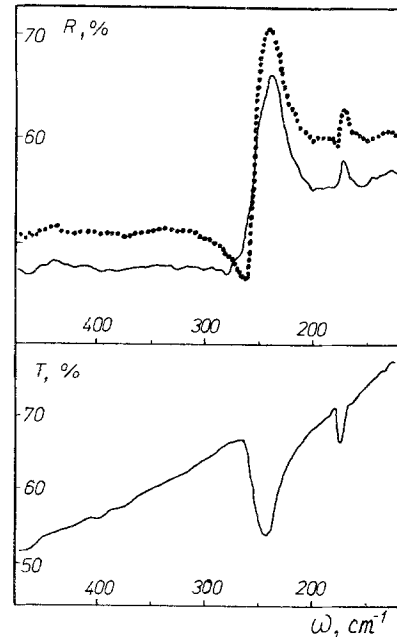


Fig. 6. Reflection coefficient  $R$  on  $\omega$  and transmittance  $T(\omega)$  for HfNiSn N° 450 at 300 K (solid line) and 77 K (dots)

for other samples (Figs. 6 and 7). These anomalies may be due to longitudinal  $\omega_{10}$  and transverse  $\omega_{10}$  optical phonons. The value of  $\omega_{10}$  is inversely proportional to the atomic mass of R atom in the RNiSn system:  $(\omega_{10}(\text{TiNiSn}) \approx 280 \text{ cm}^{-1}) > (\omega_{10}(\text{ZrNiSn}) \approx 260 \text{ cm}^{-1}) > (\omega_{10}(\text{TiNiSn}) \approx 240 \text{ cm}^{-1})$ . Considering the data on

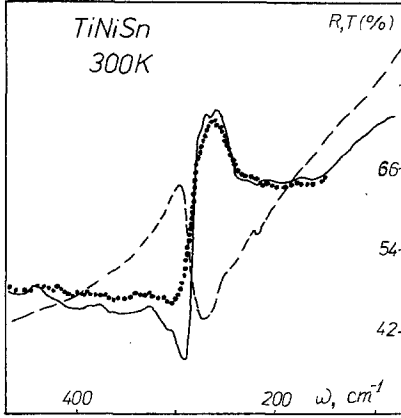


Fig. 7. Frequency dependence  $R(\omega)$  for TiNiSn N° 193 (solid line), TiNiSn N° 451 (dots) and  $T(\omega)$  for TiNiSn N° 451 (dashed line) at room temperature

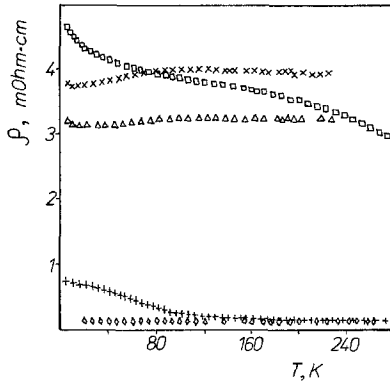


Fig. 8. Temperature dependences of resistivity  $\rho(T)$  for TiPtSn( $\diamond$ ), HfPtSn( $\times$ ), ZrPtSn( $\Delta$ ), ZrPdSn( $\square$ ) and HfPdSn( $+$ )

$R(\omega)$  over a wide  $\omega$  interval and considering the Hall coefficient, we can estimate in first approximation the effective mass of carriers  $m_1^* \approx e^2 n_H / (\epsilon_0 * \omega_{\min} (\epsilon_\infty - 1)) \approx 2m_0$  for samples with a well defined plasma minimum. For samples, which show only the phonon anomaly we estimate  $m_1^* > 2m_0$ . Here,  $\epsilon_\infty$  was estimated from the value  $R(\omega \rightarrow \epsilon_g) \approx ((\sqrt{\epsilon_\infty - 1}) / (\sqrt{\epsilon_\infty + 1}))^2$ .

The Seebeck coefficient  $S(T)$  of RNiSn ( $R = \text{Hf, Zr, Ti}$ ) is negative. It increases with temperature at  $10 < T < 200$  K almost linearly and saturates near room temperature around  $S_{\max} \approx -300 \mu\text{V/K}$ . The estimate of  $m^*$  in the strongly degenerate case from  $S(T)$  dependence gives also  $m^* \approx 2m_0$ .

It should be mentioned that transport properties, presented above, were also obtained for other materials (see Fig. 8). Crystal structure of these compounds is similar to that of RNiSn, but Ni atoms are substituted by Pt or Pd.

## Discussion

To begin a discussion it should be noted, that the resistivity of RMSn compounds is much larger than Mooij's criterion and is about the inverse minimum of metallic conductivity. Moreover, contrary to the ordinary localization models,  $\rho(T)$  increases at low  $T$  when RNiSn lattice becomes more ordered. This observation indicates that the anomalous  $\rho(T)$  behaviour in RMSn cannot be explained as a result of the Anderson localization. Instead, it suggests the existence of an energy gap in the band structure near the Fermi level. Another indication of a band gap is the extremely low (more than three orders of magnitude lower than expected for normal metals) density of carriers, obtained from the Hall effect measurements. The absence of the exponential resistivity behaviour at  $(100 < T < 300)$  K and the agreement with Mott's law at  $T < (20-30)$  K suggest the smearing out of the energy gap due to a small lattice irregularity and/or impurities.

At present we cannot give a definite answer about the origin of the energy gap at  $\epsilon_F$ . It is interesting only to point out that a recent calculation of positron annihilation probability in the MgAgAs type structure by Hanssen et al. [8] suggests the presence of deep potential pits for conduction electrons at the vacancy positions. These sharp minima might strongly influence the density of electron states in RMSn in comparison with  $\text{RM}_2\text{Sn}$ .

The electron system in RNiSn compounds is strongly interacting with the lattice of vacancies and may be described as a gas of heavy polarons. The phase transition in ZrNiSn may be due to a spontaneous change of the degree of substitution of the Zr and the Sn sublattices. This process is enhanced by the presence of the vacancies sublattice, strong electron-phonon coupling and the small difference between atomic masses of Zr and Sn. We may consider the Hall coefficient as a sum of a normal,  $R_H^0$  and an anomalous part,  $R_H^a$ , i.e.  $R_H = R_H^0 + R_H^a$ . We suppose that  $R_H^a$  increases when the degree of irregularity at room temperature of sublattices of Zr and Sn grows. In this situation the relative amplitude of the Hall effect variation  $R_H(T)/R_H(150 \text{ K})$  will be greater for less ordered samples (see Fig. 4). In TiNiSn and HfNiSn the large difference of atomic masses of Ti, Hf and Sn suppresses this transition. The vacancy system in LiAl also demonstrates a phase transition near  $T = 90$  K which is due to ordering of the Li atom's vacancies sublattice. This transition was detected from a strong kink in the  $R_H(T)$  dependence [9] and from an anomaly in the heat capacity [3].

In conclusion, the results presented here as well as the data published earlier by Aliev et al. [10,11]

and Palstra et al. [12] show that the formation of the vacancy lattice leads to a qualitative transformation of the energy spectrum in the vicinity of the Fermi level.

We would like to acknowledge helpful discussions with I.P. Zvyagin and B.L. Altshuler and also to thank A.V. Andreev and Yu.V. Stadnik for their assistance in the experiment.

## References

1. Bernard, J.E., Zunger, A.: *Phys. Rev. B* **37**, 6835 (1988)
2. Jorgensen, J.D., Beno, M.A., Hinks, D.G., Soderholm, L., Volin, K.J., Hitterman, R.L., Grace, J.D., Schuller, I.K., Serge, C.U., Zhang, K., Kleefisch, M.S.: *Phys. Rev. B* **36**, 3608 (1987)
3. Kuriyama, K., Yanada, S., Nozaki, T., Kamijoh, T.: *Phys. Rev. B* **24**, 6158 (1981)
4. Campbell, C.C.M.: *J. Phys. F* **5**, 1931 (1975)
5. Helmholdt, R.B., Groot, R.A., Mueller, F.M., Engen, P.G., Buschow, K.H.J.: *J. Magn. Magn. Mater.* **43**, 249 (1984)
6. Groot, R.A., Mueller, F.M., Engen, P.G., Buschow, K.H.J.: *Phys. Rev. Lett.* **50**, 2024 (1983)
7. Scolozdra, R.V., Stadnik, U.V., Starodinova, E.E.: *Ukr. Fis. Zh.* **31**, 720 (1986)
8. Hanssen, K.E.H.M., Mijnders, P.E.: *Phys. Rev. B* **34**, 5009 (1986)
9. Kuriyama, K., Nozaki, T., Kamijoh, T.: *Phys. Rev. B* **24**, 2235 (1982)
10. Aliev, F.G., Brandt, N.B., Kozyrkov, V.V., Moshchalkov, V.V., Scolozdra, R.V., Stadnik, U.V.: *Fiz. Niz. Temp.* **12**, 498 (1987)
11. Aliev, F.G., Brandt, N.B., Kozyrkov, V.V., Moshchalkov, V.V., Scolozdra, R.V., Stadnik, U.V., Pecharskii, V.K.: *Pis'ma Zh. Eksp. Teor. Fiz.* **45**, 535 (1987)
12. Palstra, T.T.M., Nieuwenhuys, G.J., Mydosh, J.A., Bushow, K.H.J.: *J. Magn. Magn. Mater.* **54-57**, 551 (1986)

F.G. Aliev, N.B. Brand, V.V. Moshchalkov, V.V. Kozyrkov,  
 R.V. Skolozdra, A.I. Belogorokhov  
 Low Temperature Physics Laboratory  
 Physics Department  
 Moscow State University  
 SU-117234 Moscow  
 USSR